Possibility of detecting forest fires from space during daytime under conditions of broken clouds. Part 2. Numerical experiment

***V.G. Astafurov and V.V. Belov**

Institute of Atmospheric Optics,
Siberian Branch of the Russian Academy of Sciences, Tomsk
**Tomsk University of Control Systems and Radio Electronics*

Received November 20, 2000

We present a statistical model of the total power of the background over the spectral range from 3.55 to 3.93 μm developed for use in problems on detecting from space the places of forest fire ignition under conditions of broken clouds during day and night. Two types of approximations for the probability density of background power: the Laguerre polynomials and Pearson curves are considered. Based on the closed numerical experiment within the Neumann-Pearson criterion the probabilities of fire detection are found. The results obtained show the principle possibility of early fire detection from the space under conditions of broken clouds.

Introduction

Detection of places of fire ignition (PFI) from space by IR radiation is performed against the background of disturbances caused by solar radiation reflected from the system "cloudy atmosphere–underlying surface" and the thermal radiation of the underlying surface (US), clouds, and atmosphere. A possibility of early PFI detection from space by IR radiation at night under conditions of broken clouds has been considered in Refs. 1 and 2. In Ref. 3 the algorithm and calculated results on the statistical characteristics of the disturbance due to solar radiation and total day background over the spectral range 3.55–3.93 μm is presented. The effectiveness of PFI detection is estimated by the magnitude of the signal-to-noise ratio. Note that these estimations have a purely qualitative character since they do not use any specific criterion of detection. Based on the results obtained earlier in this paper a statistical model of the total background power $p = p_S + p_{IR}$ recorded with a radiometer in the spectral range 3.55–3.93 μm during day and night is proposed in application to problem on PFI detection. Here p_S and p_{IR} are the power of the disturbance due to solar radiation and thermal radiation noise. Two types of approximations of histograms of the total background power and disturbance of solar radiation are considered, namely, the Laguerre polynomials and Pearson curves. In the second part of the paper the probabilities of detecting PFI calculated by use of Neumann-Pearson criterion based on the results of closed numerical experiment are presented.

Statistical model

It has been proposed in Ref. 1 to use the Laguerre series to approximate the probability density $f_0(p)$. In this case the component of the background due to thermal radiation has only been considered. Let us extend this approach to daytime conditions of measurement in the presence of a disturbance due to solar radiation. In the case when only two moments, i.e., the mean power of the background $\langle p \rangle$ and its variance $D(p)$ are known, the approximation by the Laguerre series coincides with the gamma-distribution

$$f_0(p) = \frac{1}{\eta\Gamma(\nu + 1)} \left(\frac{p}{\eta}\right)^{\nu} \exp\left(-\frac{p}{\eta}\right), \qquad (1)$$

whose parameters are determined by expressions

$$\nu = \frac{\langle p \rangle^2}{D(p)} - 1; \quad \eta = \frac{D(p)}{\langle p \rangle}. \qquad (2)$$

To estimate the accuracy of the approximation (1) in the expansion of $f_0(p)$ over Laguerre polynomials, it is necessary to take into account an added term of the series. It can be shown[1] that in this case $f_0(p)$ has the following form:

$$f_0(p) = \frac{1}{\eta}\left(\frac{p}{\eta}\right)^{\nu} \exp\left(-\frac{p}{\eta}\right)\left[\frac{1}{\Gamma(\nu + 1)} + c_3 L_3^{(\nu)}\left(\frac{p}{\eta}\right)\right], \qquad (3)$$

where

$$6L_3^{(\nu)}(x) = (\nu + 1)(\nu + 2)(\nu + 3) - 3x(\nu + 2)(\nu + 3) + 3x^2(\nu + 3) - x^3$$

is the Laguerre polynomial of the third power,

0235-6880/01/02 141-05 $02.00

$$c_3 = \frac{(\nu + 1)(\nu + 2)(\nu + 3)}{\Gamma(\nu + 4)} (1 - \xi_\gamma); \qquad (4)$$

$$\xi_\gamma = \langle p^3 \rangle / \langle p^3 \rangle^{(\gamma)}; \qquad (5)$$

$\langle p^3 \rangle$ is the third initial moment of the total background power which is calculated by a histogram,

$$\langle p^3 \rangle^{(\gamma)} = \eta^3(\nu + 1)(\nu + 2)(\nu + 3)$$

is the third initial moment of the gamma-distribution (1). One can see from the expressions (4) and (5) that the difference $(1 - \xi_\gamma)$ equals to the value of relative deviation of $\langle p^3 \rangle^{(\gamma)}$ from $\langle p^3 \rangle$. Therefore $|1 - \xi_\gamma|$ can be considered as some modulus of precision of the approximation of $f_0(p)$ by the gamma-distribution at the level of third moments. Giving a value of the maximally admissible deviation of ξ_γ from the unit, we can find the fields of applicability of the approximations (1) and (3).

As in Ref. 3, all our calculations relate to the spectral subrange from 3.6 to 3.8 μm for sounding along nadir. In this case the earlier accepted notations are used: ε_λ is the emission power of the US at the wavelength λ, $\xi_\odot$ is the zenith angle of the Sun. Figures 1 and 2 show the dependences of the parameters ν and η on the cloud amount N for nighttime and daytime conditions, respectively.

Figure 1 also presents the dependence of ξ_γ on N. The calculated results show that for measurements during nighttime the inequality $|1 - \xi_\gamma| < 0.05$ is satisfied, and at daytime it is $|1 - \xi_\gamma| < 0.003$. Based on these facts we can draw a conclusion that the approximation of the probability density for the total background power $f_0(p)$ by the gamma-distribution has a sufficiently high degree of accuracy at the level of the third initial moments.

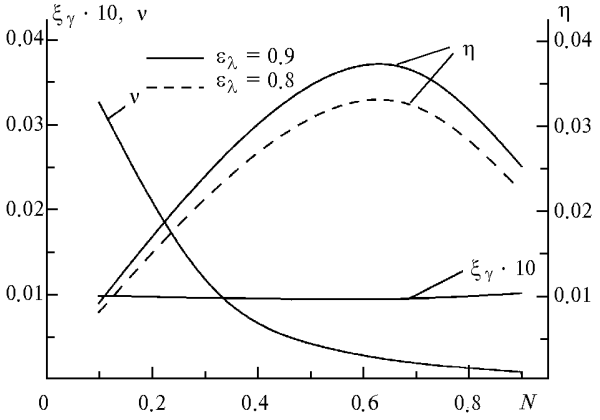

Fig. 1. Dependence of the gamma-distribution parameters and value of the ratio ξ_γ on the cloud amount N at night.

In the problem of PFI detection the disturbance due to solar radiation is of no importance. However, if it is necessary, the parameters ν and η for its approximation can be found with the expressions (2). The average power of the disturbance produced by solar radiation $\langle p_S \rangle$ and the value of its relative standard deviation as functions of the cloud amount are shown in Fig. 2 in Ref. 3. The calculated results on the dependence ξ_γ are presented in Fig. 3. One can see from these dependences that at certain values of the parameters the deviation $f_0(p_S)$ from the gamma-distribution can be significant. For example, for $\varepsilon_\lambda = 1$ and $N = 0.3$ (curves *1* and *3* in Fig. 3) we have $|1 - \xi_\gamma| = 0.12$. In this case it is expedient to increase the number of terms in the Laguerre series and to use for $f_0(p_S)$ the approximation (3).

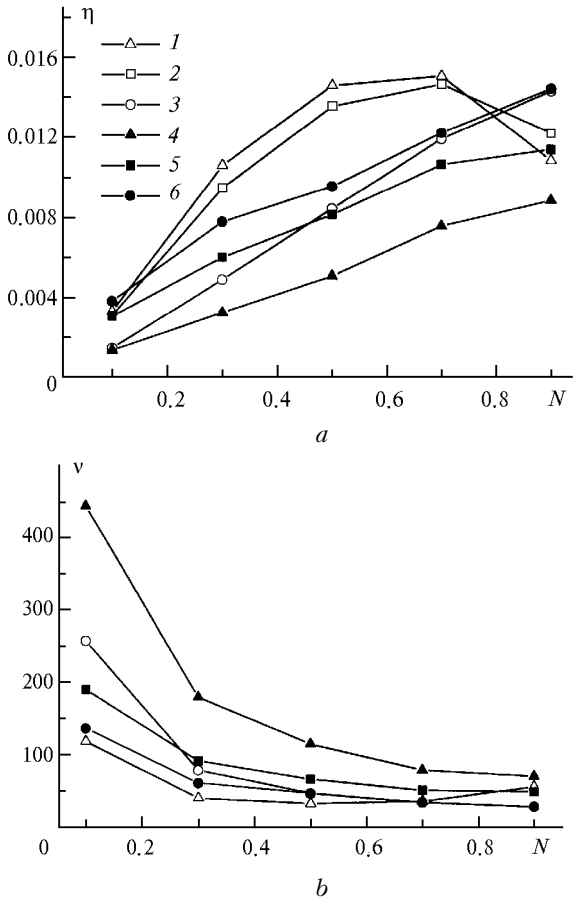

Fig. 2. Dependences of the parameters η (*a*) and ν (*b*) on the cloud amount N for the gamma-distribution of the total background power: $\varepsilon_\lambda = 1$, $\xi_\odot = 10°$ (curve *1*); $\varepsilon_\lambda = 1$, $\xi_\odot = 20°$ (*2*); $\varepsilon_\lambda = 1$, $\xi_\odot = 40°$ (*3*); $\varepsilon_\lambda = 0.9$, $\xi_\odot = 10°$ (*4*); $\varepsilon_\lambda = 0.9$, $\xi_\odot = 20°$ (*5*); $\varepsilon_\lambda = 0.9$, $\xi_\odot = 40°$ (*6*).

The use of approximation of $f_0(p)$ by the Laguerre polynomials is overburdened by a large number of series terms. It is also necessary here to take into account that for the approximated expressions of the type (3) the normalization condition is not always satisfied, i.e., $\int f_0(p)\mathrm{d}p \neq 1$. It is especially true in the "tails" of the distributions at large values of p. At the same time it is exactly these regions that are important in determining the thresholds in the detection problems.

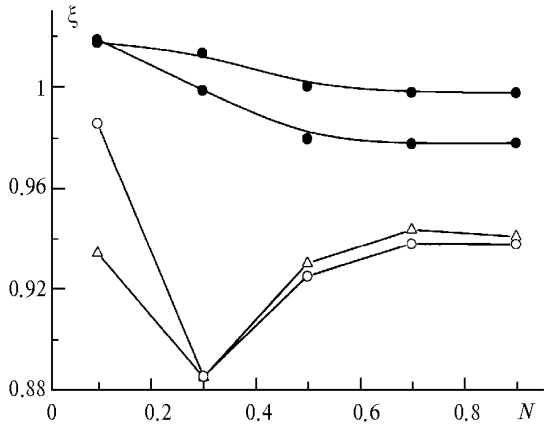

Fig. 3. Dependence of the parameter ξ_γ on the cloud amount N at the presence of the disturbance due to solar radiation. Notations are the same as in Fig. 2.

Another method to choose the approximations is connected with the use of distributions of the Pearson family.[4] In this case the shape of the curve depends on the values of the following parameters:

$$\beta_1 = \mu_3^2/\mu_2^3 = \gamma_1^2 \quad \text{and} \quad \beta_2 = \mu_4/\mu_2^2 = \gamma_2 + 3, \qquad (6)$$

here μ_i is the central moment of the ith order, γ_1 and γ_2 are the coefficients of asymmetry and kurtosis. If we draw the point with coordinates (β_1, β_2) at the diagram of distributions of the Pearson families, then we can determine the type of the curve. The diagram mentioned can be found in the monograph 4. Central moments μ_i were calculated using histograms of the background power and the disturbance due to solar radiation, which were calculated by the method of numerical simulation. One can find examples of such histograms in Ref. 3.

Table 1. Types of distributions of the Pearson family for the disturbance due to solar radiation

N	$\varepsilon_\lambda = 1$			$\varepsilon_\lambda = 0.9$		
	$\xi_\odot = 10°$	$\xi_\odot = 20°$	$\xi_\odot = 40°$	$\xi_\odot = 10°$	$\xi_\odot = 20°$	$\xi_\odot = 40°$
0.1	I(J)	I(J)	I(J)	I(J)	I(J)	IV
0.3	I(J)	I(J)	I(J)	I(J)	I	I
0.5	I	I	I	I	I	I
0.7	I	I	I	I	I	I
0.9	I	I	I	I	I	I

Table 2. Types of distributions of the Pearson family for the total background power and the nighttime conditions of measurements at $\varepsilon_\lambda = 0.9$

N	0.1	0.3	0.5	0.7	0.9
Type	I(J)	I	I	I	I(J)

Results of the choice of approximations from the family of Pearson curves for various measurement conditions, values of the cloud amount N, and parameters ε_λ and $\xi_\odot$ are presented in Tables 1, 2, and 3. One can see from these tables that the distributions of I, I(J), and IV types for daytime conditions (Table 3) have proved to be suitable. To approximate the histograms of the disturbance due to solar radiation and total background power under nighttime conditions, we can restrict ourselves to the distributions of two types: I and I(J) (Tables 1 and 2). Here the classification assumed in Ref. 4 is used, in accordance with this classification I and I(J) denote the beta-distribution and its J-shape form. These probability densities differ by the values of their parameters.

Probability density of the beta-distribution has the following form:

$$f_0(p) = \frac{\Gamma(a+b)}{\Gamma(a)\Gamma(b)}\, p^{a-1}(1-p)^{b-1},\ 0 < p < 1 \qquad (7)$$

with the parameters

$$a = \frac{m_1(m_1 - m_2)}{m_2 - m_1^2};\quad b = \frac{(1-m_1)(m_1 - m_2)}{(m_2 - m_1^2)},$$

where m_i is the initial moment of the background power of the ith order, the condition $0 < p < 1$ does not impose any principle restrictions. Expression for the probability density distribution of the IVth type has the form

$$f_0(X) = c(X^2 + A^2)^{1/2b_2} \exp\left(-\frac{B}{Ab_2}\arctan\frac{X}{A}\right), \qquad (8)$$

where

$$X = p + \frac{b_1}{2b_2};\quad B = b_1\left(1 + \frac{1}{2b_2}\right);\quad A^2 = \frac{b_0}{b_2} - \frac{b_1}{4b_2^2};$$

$$-\infty < x < \infty,\quad b_i = c_i/d;$$

$$c_0 = -\mu_2(4\mu_2\mu_4 - 3\mu_3^2),\quad c_1 = \mu_3(\mu_4 + 3\mu_2^2),$$

$$c_2 = -2\mu_2\mu_4 + 6\mu_2^3 + 3\mu_3^2;\quad d = 10\mu_2\mu_4 - 18\mu_2^3 - 12\mu_3^2.$$

Note that the proposed methods of approximation do not contradict each other. It is connected with that the gamma-distribution at the Pearson diagram corresponds to the distribution of III type, and the points corresponding to it lie on the boundary of the region related to the beta-distribution.

Table 3. Types of distributions of the Pearson family for the total background power and the daytime conditions of measurements

N	$\varepsilon_\lambda = 1$			$\varepsilon_\lambda = 0.9$			$\varepsilon_\lambda = 0.8$		
	$\xi_\odot = 10°$	$\xi_\odot = 20°$	$\xi_\odot = 40°$	$\xi_\odot = 10°$	$\xi_\odot = 20°$	$\xi_\odot = 40°$	$\xi_\odot = 10°$	$\xi_\odot = 20°$	$\xi_\odot = 40°$
0.1	I(J)	I(J)	IV	IV	I	I(J)	I(J)	I(J)	I(J)
0.3	I(J)	I(J)	IV	IV	IV	I	I	I	I
0.5	I	I	I	IV	IV	V	I	I	I
0.7	I	I	I	IV	IV	IV	I	I	I
0.9	I	I	I	I	I	I	I	I	I

The approximations obtained can be used to determine the probability density $f_1(p_\Sigma)$ of the total power of PFI radiation and the background $p_\Sigma = p + p_{fl}$ (p_{fl} is the recorded power of the PFI radiation). It is shown in Ref. 2 that for the pointwise PFI

$$f_1(p_\Sigma) = n(\theta) f_0(p_\Sigma) + [1 - n(\theta)] f_0(p_\Sigma - p_{f0}), \quad (9)$$

where $n(\theta)$ is the probability of screening the line of sighting toward a PFI by clouds, θ is the angle between the line of sighting and nadir, p_{f0} is the PFI radiation power recorded with a radiometer, if not screened by clouds. The probability $n(\theta)$ depends on the height of cloud layer and the shape of clouds. It is clear that for sounding along nadir we have $n(0) = N$. Substituting the chosen approximation for $f_0(p)$ in expression (9) we obtain the expression for the probability density $f_1(p_\Sigma)$.

Effectiveness of the PFI detection

Let us consider the single-channel PFI detector that uses, as an initial information, the IR radiation recorded with a radiometer over the spectral range from 3.55 to 3.93 μm. Let us remind that the radiation maximum for the characteristic temperatures of forest fires, which lie in the interval 800–1000 K, is in this range. The scheme of the PFI detection is shown in Fig. 1 in Ref. 3. Analysis of the effectiveness of the single-channel detector allows us to address the principle question: is it possible to detect PFI under conditions of broken clouds, and what its effectiveness will be in this case? It is clear that if one simultaneously conducts measurements in other spectral ranges, the quality of detection can only be improved. For example, the spectral range from 10.3 to 11.3 μm is normally used to take into account the fluctuations of the emission power of the Earth's surface.

Fluctuations of the power recorded under conditions of broken clouds dominate compared with the internal noise of the optical receiver of a radiometer. Therefore considering the characteristics of the effectiveness we can neglect this noise. Thus, the initial information necessary for making a decision on the presence of PFI in the radiometer field of view is the power p recorded by a radiometer over the spectral interval from 3.55 to 3.93 μm. In Ref. 1 the use of Neumann-Pearson criterion to detect PFI was substantiated and two hypotheses were determined: H_0 – PFI absents in the radiometer field of view, H_1 – PFI presents there. Since the mean values of the power p in the hypotheses H_0 and H_1 satisfy an obvious condition $\langle p \rangle_1 > \langle p \rangle_0$ (here indices denote the numbers of hypotheses), the whole interval of possible values of p is divided by the threshold u_α into two intervals: $[0, u_\alpha]$ and $(u_\alpha, +\infty)$. Decisions are made according to the following rule: γ_0 (PFI absents) if $p \in [0, u_\alpha]$ and γ_1 (PFI presents) if $p \in (u_\alpha, +\infty)$. The value of the threshold u_α is found for the given probability of false alarm α from the equation

$$\alpha = \int_{u_\alpha}^{+\infty} f_0(p) \mathrm{d}p, \quad (10)$$

and the probability of correct detection equals to

$$1 - \beta = \int_{u_\alpha}^{+\infty} f_1(p) \mathrm{d}p. \quad (11)$$

As was noted above, the distribution $f_0(p)$ is determined by the statistical characteristics of the background only and does not depend on the radiation power from the place of the fire ignition for $P(\Delta\lambda)$ in the spectral range $\Delta\lambda$ chosen.

To calculate the characteristics of PFI detection, it is necessary to know its area S_{fl} and corresponding distribution of temperature T_{fl}, which depends on the composition of forest combustible materials, humidity, type of forest fire, and a set of other factors.[5] We will consider the characteristics of early detection of places of ignition, for which the condition $S_{fl} \ll S_0$ is satisfied. Here S_{fl} is the PFI area, S_0 is the area of the section of earth's surface which lies in the radiometer field of view. Since the radiometer determines some mean temperature of the US section, for $S_{fl} \ll S_0$ we can use a simplest model of PFI with the constant temperature. For calculations we will assume $T_{fl} = 1000$ K.[5] Temperature of the US out of the fire equals to 300 K. Tables 4–6 give the calculated results on the probabilities of PFI detection $1-\beta$ are presented for the nighttime and daytime conditions and sounding along nadir, $S_{fl} = 100$ m^2 and $S_{fl} = 400$ m^2. To determine the value of the threshold u_α and probability of correct detection $1-\beta$ by the formulae (10) and (11), the methods of numerical integration of corresponding histograms were used. If the probability of false alarm is $\alpha = 0$, then the threshold value corresponds to the maximum level of the background, and a detector does not give false alarm on the presence of a PFI.

Table 4. The probability of detecting a place of fire ignition $1-\beta$ by the Neumann-Pearson criterion under nighttime conditions

N	$\varepsilon_\lambda = 0.9$		$\varepsilon_\lambda = 0.8$	
	$S_{fl} = 100$ m^2	$S_{fl} = 400$ m^2	$S_{fl} = 100$ m^2	$S_{fl} = 400$ m^2
	$\alpha = 0$			
0.1	0.90	0.91	0.91	0.92
0.3	0.69	0.73	0.70	0.74
0.5	0.48	0.53	0.49	0.55
0.7	**0.27**	0.34	**0.28**	0.36
0.9	**0.082**	0.16	**0.089**	0.17
	$\alpha = 0.1$			
0.1	0.90	0.91	0.91	0.92
0.3	0.77	0.76	0.71	0.74
0.5	0.62	0.67	0.53	0.58
0.7	0.43	0.50	0.37	0.43
0.9	0.25	0.32	0.27	0.34
	$\alpha = 0.2$			
0.1	0.90	0.91	0.91	0.92
0.3	0.71	0.74	0.72	0.76
0.5	0.53	0.58	0.56	0.61
0.7	0.40	0.46	0.43	0.48
0.9	0.34	0.41	0.38	0.44

Table 5. The probability of detecting a place of fire ignition $1-\beta$ by the Neumann-Pearson criterion under daytime conditions for the zenith angle of the sun $\xi_\odot = 10°$

N	$\varepsilon_\lambda = 0.9$				$\varepsilon_\lambda = 0.8$			
	$\alpha = 0$		$\alpha = 0.1$		$\alpha = 0$		$\alpha = 0.1$	
	$S_{fl} = 100$ m^2	$S_{fl} = 400$ m^2	$S_{fl} = 100$ m^2	$S_{fl} = 400$ m^2	$S_{fl} = 100$ m^2	$S_{fl} = 400$ m^2	$S_{fl} = 100$ m^2	$S_{fl} = 400$ m^2
0.1	0.89	0.91	0.92	0.932	0.89	0.90	0.90	0.91
0.3	0.70	0.72	0.70	0.73	0.67	0.74	0.71	0.75
0.5	0.28	0.54	0.51	0.56	0.37	0.54	0.53	0.58
0.7	**0.044**	0.34	**0.35**	0.4250	**0.091**	0.33	**0.39**	0.46
0.9	**0.0081**	0.16	**0.25**	0.34	**0.013**	0.15	**0.22**	0.32

Table 6. The probability of detecting a place of fire ignition $1-\beta$ by the Neumann-Pearson criterion under daytime conditions at the probability of false alarm $\alpha = 0.2$

N	$\varepsilon_\lambda = 0.9$				$\varepsilon_\lambda = 0.8$			
	$\xi_\odot = 10°$		$\xi_\odot = 40°$		$\xi_\odot = 10°$		$\xi_\odot = 40°$	
	$S_{fl} = 100$ m^2	$S_{fl} = 400$ m^2	$S_{fl} = 100$ m^2	$S_{fl} = 400$ m^2	$S_{fl} = 100$ m^2	$S_{fl} = 400$ m^2	$S_{fl} = 100$ m^2	$S_{fl} = 400$ m^2
0.1	0.92	0.939	0.91	0.92	0.90	0.91	0.88	0.91
0.3	0.78	0.81	0.75	0.78	0.72	0.75	0.69	0.75
0.5	0.66	0.73	0.63	0.67	0.55	0.61	0.58	0.63
0.7	0.53	0.59	0.50	0.56	0.45	0.51	0.44	0.52
0.9	0.35	0.42	0.33	0.40	0.31	0.40	0.32	0.39

The calculated results on the probabilities for sounding along nadir ($\theta = 0$), which are presented in tables, allow us to draw the following conclusions on the effectiveness of PFI detection within the accepted model of cloud field:

1. The probabilities of PFI detection depend negligibly on the emission power of the US and zenith angle of the Sun (Table 6). It contradicts slightly to the results on a decrease of the ratio $\mathrm{SNR} = \langle p_\Sigma \rangle / \sqrt{D(p_\Sigma)}$ with the growth of the Sun zenith angle $\xi_\odot$ which were obtained earlier.[3] The value of SNR was used to estimate the effectiveness of PFI detection. The contradiction mentioned can be explained by that the SNR depends on the variance of the total power of PFI radiation and background only, whereas the behavior of $f_0(p)$ at "large values" of p, on which the threshold u_α depends, is determined by the moments of distribution of higher orders;

2. Given the values of the false alarm probability $\alpha = 0.1$ and $\alpha = 0.2$, we can obtain sufficiently high (in our opinion) effectiveness of PFI detection having the dimensions 10×10 m at large values of the cloud amount N. Moreover, the value $1 - \beta$ exceeds the probability of the PFI falling into the gap between clouds which equals to $1 - N$. It testifies to the detection of PFI which are closed by optically thin edges of clouds (Table 4);

3. High effectiveness of detecting the PFI having the dimensions of 20×20 m is associated with that the PFI is partially observed through the cloud gaps (Tables 4, 5, and 6);

4. Owing to a high level of the disturbance due to solar radiation, the probability of detection of PFI with the dimensions of 10×10 m at $\alpha = 0$ is essentially lower than the probability of observing the PFI in cloud gaps, which equals to $1 - N$ (see boldface numbers in Table 5). Corresponding probabilities of PFI detection at night are considerably higher (see boldface numbers in Table 4). Increase of the probability of false alarm α causes an essential increase in the effectiveness of detection under daytime conditions. Corresponding probabilities are presented in boldface cells of Table 5.

The results obtained show that in principle early PFI detection from space is possible under conditions of broken clouds at different times whole day round. Realization of this possibility is associated with the development of algorithms for finding current value of the threshold u_α from data of satellite observations. It is expedient to consider also the use of multi-spectral measurements that must essentially increase the effectiveness of PFI detection under conditions of broken clouds.

References

1. V.G. Astafurov and G.A. Titov, Atmos. Oceanic Opt. **9**, No. 5, 409–414 (1996).
2. V.G. Astafurov, Atmos. Oceanic Opt. **12**, No. 3, 251–256 (1999).
3. V.G. Astafurov, Atmos. Oceanic Opt. **13**, No. 4, 326–330 (2000).
4. V.I. Tikhonov, *Statistical Radio Engineering* (Radio i Svyaz', Moscow, 1982), 624 pp.
5. A.M. Grishin, *Physics of Forest Fires* (Tomsk State University, Tomsk, 1994), 218 pp.